

R.J. Scheck  
C. Kubitzek  
R. Hierner  
U. Szeimies  
T. Pfluger  
K. Wilhelm  
K. Hahn

## The scapholunate interosseous ligament in MR arthrography of the wrist: correlation with non-enhanced MRI and wrist arthroscopy

**Abstract Objective.** To compare three-compartment MR wrist arthrography with non-enhanced MRI in correlation with wrist arthroscopy, and to evaluate the potential of MR arthrography for consistently visualizing all parts of the scapholunate interosseous ligament of the wrist (SLIL) and exactly diagnosing the site and extent of SLIL defects.

**Design and Patients.** In 41 patients with wrist pain (34 patients with wrist pain for more than 6 months) plain radiographs, stress views, non-enhanced MRI and three-compartment MR arthrography were done within 2 h of each other, using three-dimensional volume acquisition (0.6–1.0 mm effective slice thickness) with a gradient-recalled echo sequence and a 1.5-T magnet. The MR arthrography findings were compared with the findings from non-enhanced MRI and correlated with the arthroscopic findings in all patients.

**Results.** The dorsal, central and palmar segments of the SLIL could be delineated exactly by MR arthrography in 95% of the patients; with non-

enhanced MRI only 28% of SLIL segments were seen consistently. Demonstration of SLIL defects was possible with high diagnostic confidence in 42% of SLIL segments by non-enhanced MRI and in 94% by MR arthrography. With wrist arthroscopy as the standard of reference, sensitivity and specificity values for SLIL perforations were 52%/34% for non-enhanced MRI and 90%/87% for MR arthrography. **Conclusions.** MR arthrography, using three-dimensional volume acquisition with thin slices (0.6–1.0 mm), combines the advantages of three-compartment arthrography and non-enhanced MRI. It shows the precise location and magnitude of ligamentous defects of all parts of the SLIL, correlates well with wrist arthroscopy and has potential implications for diagnosis and treatment planning.

**Key words** Arthrography, three-compartment · Ligaments, MRI · MRI, arthrography · Scapholunate interosseous ligament · Wrist, arthrography

R.J. Scheck, M.D. (✉) · C. Kubitzek  
U. Szeimies, M.D. · T. Pfluger, M.D.  
K. Hahn, M.D.  
Department of Radiology,  
Klinikum Innenstadt,  
Ludwig-Maximilian-University Munich,  
Ziemssenstrasse 1,  
D-80366 Munich, Germany

R. Hierner, M.D. · K. Wilhelm, M.D.  
Department of Hand Surgery,  
Klinikum Innenstadt,  
Ludwig-Maximilian-University,  
Munich, Germany

### Introduction

The scapholunate interosseous ligament (SLIL) is an important biomechanical element between the proximal carpal bones and contributes to the function and stability of the entire wrist [1]. It is essential for smooth translation of the scaphoid relative to the lunate and normal wrist function is not possible without it [2]. An exact di-

agnosis of SLIL defects considering the three histologically and biomechanically different parts (dorsal, central and palmar segments) of the ligament is necessary for planning reconstructive surgical procedures, particularly dorsal capsulodesis techniques or even palmar surgical techniques for ligamentous repair [3].

Confusion exists about the clinical and therapeutic implications of an SLIL leakage in conventional arthro-

raphy [4, 5]. From previous MRI studies investigating the appearance of the normal SLIL it is not clear which SLIL patterns are pathological in MRI [1, 6]. It is generally agreed that from a biomechanical point of view stability of the SLIL originates predominantly from its intact dorsal and palmar parts and that an isolated perforation of the central membranous portion of the ligament does not lead to instability [7]. Therefore it may be essential to know the exact site and size of SLIL defects [8, 9] in order to plan adequate treatment.

Three-compartment MR arthrography is a method of obtaining multidirectional images of wrist pathology. It can delineate wrist ligaments directly with high spatial and contrast resolution [8, 10, 11]. Thus MR arthrography has great potential to determine exactly the location and magnitude of defects and even to show elongated and scarred ligaments [5, 11].

The goals of this study were to (a) describe the signal intensity characteristics of the SLIL in non-enhanced MRI, (b) compare non-enhanced MRI and MR arthrography for delineation of SLIL segments, (c) evaluate the advantages of MR arthrography over non-enhanced MRI and (d) investigate the potentials of MR arthrography for showing the exact location and extent of SLIL defects as compared with wrist arthroscopy in 41 patients with (mainly chronic) wrist pain.

## Patients and methods

### Patients

The study group comprised 41 patients (18 female, 23 male; average age 34 years) with wrist pain, mainly chronic in character (34 patients had wrist pain for longer than 6 months), but generally (39/41) without radiographic evidence of instability as diagnosed by bilateral static, motion and stress views. They were examined between February 1994 and April 1996 by non-enhanced MRI, conventional three-compartment wrist arthrography and MR arthrography.

Before MR examination each patient had posteroanterior and lateral radiographs in neutral position, radial/ulnar deviation and flexion/extension views done bilaterally. Under fluoroscopic control additional posteroanterior (with the scapholunate joint profiled) and lateral stress views were taken of the painful wrist in dorsal/palmar flexion and ulnar/radial deviation.

The study was approved by the ethics committee of our university and informed consent was obtained from all patients.

### MRI

All MRI was done with a 1.5-T MR system (Magnetom SP 63, Siemens, Erlangen, Germany) and a dedicated transmit-receive wrist imaging coil (8 cm×8 cm; Siemens, Erlangen, Germany).

Patients were placed in the prone position with their wrist overhead, the elbow extended to 180°, and a soft support under the chest to avoid hyperextension of the shoulder. The wrist was fixed, ulnar side down, in the center of the coil. To evaluate wrist ligaments, imaging was performed in a sagittal (corresponding to the usual coronal) plane. A T1-weighted gradient-echo three-dimensional (GE 3D) sequence with 12 cm field of view and 0.6–1.0

mm effective slice thickness (TR 60, TE 10, flip angle 20°, 1 acquisition, matrix 256×256) was used in all patients.

### Arthrography

Conventional wrist arthrography was performed on the same day, after the MR examination. A solution of Isovist (Schering, Berlin, Germany) and Magnevist (Schering, Berlin, Germany) was prepared as follows: 0.05 ml of Magnevist was mixed with 10 ml of Isovist (Magnevist : Isovist=1:200). Under radiographic control a 24-G needle was introduced with aseptic technique into the mid-carpal joint between the scaphoid, capitate and trapezoid bones to inject the prepared contrast medium until the joint was fully distended and the patient reported a tense feeling in the wrist. Under fluoroscopic control radiographs were obtained during injection of contrast medium as well as during and after exercise maneuvers (palmar/dorsal flexion, radial/ulnar deviation and axial compression) in posteroanterior projections to show leakage of contrast medium from the mid-carpal into the radiocarpal joint. Any site of communication through the SLIL was determined and recorded. Directly after this the distal radioulnar joint and then the radiocarpal joint were injected accordingly, unless these compartments were already distended by contrast medium. Other sites of communicating defects were recorded, which could be the subject of another report. The three-compartment arthrography was accomplished within 20–30 min.

### MR arthrography

MR arthrography was performed within 30 min of three-compartment arthrography. A T1-weighted GE 3D sequence with 0.6–1.0 mm effective slice thickness (TR 30, TE 10, flip angle 70°, 1 acquisition, matrix 256×256) and 12-cm field of view was applied in the sagittal plane.

### Interpretation

The evaluation was done jointly by two observers experienced in the diagnosis of wrist pathology, separately for the three different parts of the SLIL [dorsal, central (=scapholunate membrane) and palmar thirds of the ligament] for the sagittal non-enhanced and MR arthrography volume acquisition images. The observers (R.S., C.K.) were not aware of the clinical, arthrographic and surgical findings.

For non-enhanced and enhanced MR images the number of sections was counted in which the SLIL was seen and calculated (in millimeters) as the dorsopalmar extension of the SLIL.

Signal intensity characteristics (type 1–5) were evaluated according to Smith [1] for non-enhanced MRI: absent signal intensity (type 1), central intermediate signal intensity (type 2), linear intermediate signal intensity traversing the distal surface only (type 3), linear intermediate signal intensity traversing the proximal surface only (type 4) or linear intermediate signal intensity traversing both the proximal and distal surfaces of the SLIL (type 5).

Detectability of the SLIL on non-enhanced MRI and MR arthrography images was assessed using a three-point scale: 1, good delineation; 2, intermediate delineation; 3, poor delineation.

For diagnostic confidence (non-enhanced MRI, MR arthrography) a five-point scale was used: 1, certainly normal; 2, probably normal; 3, no assessment possible; 4, probably pathological; and 5, certainly pathological.

Imaging findings were correlated with wrist arthroscopy as the standard of reference. Radiocarpal arthroscopy was done in 41 patients, additional mid-carpal arthroscopy in 19 patients.

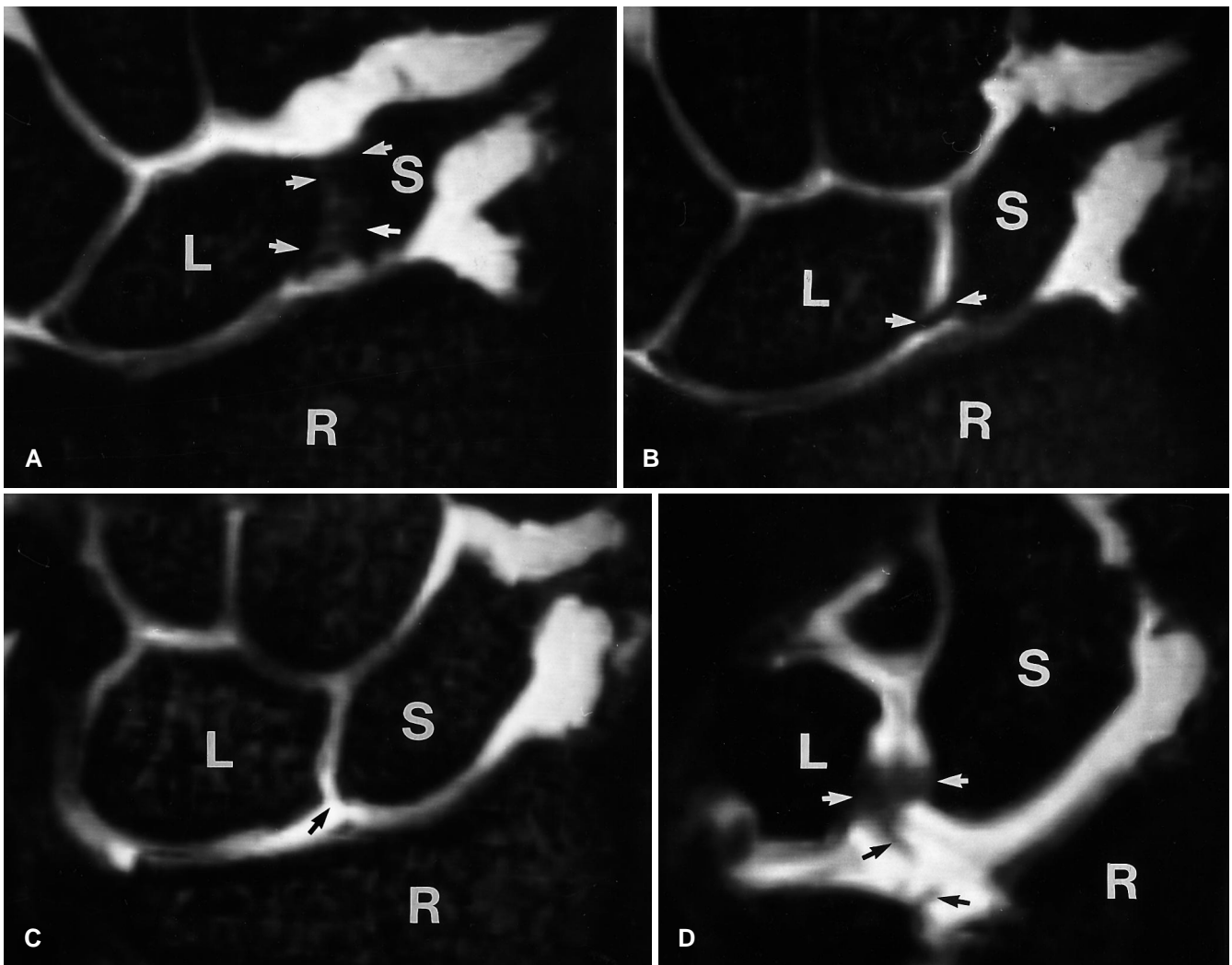


**Fig. 1A–D** A 29-year-old man with mid-carpal pain for 2 years. Arthrography, obtained after a mid-carpal injection, shows a very slow leakage of contrast material through the scapholunate interosseous ligament (SLIL) into the radiocarpal joint. Postarthrography three-dimensional gradient-echo images with 0.7 mm effective slice thickness are shown. **A** The dorsal segment of the SLIL is intact. It consists of taut, transversely orientated collagen fascicles which insert into the scaphoid and lunate bones (*arrows*) [7, 8]. **B** The central part of the SLIL (*arrows*), which is a fibrocartilaginous membrane, is 0.8 mm thick and appears intact in this slice. **C** Thin section 2 mm more palmar than **B** demonstrates leakage of Gd-DTPA between the carpal and the radiocarpal joint. The pinhole defect (*arrow*) through the interosseous membrane has a dorsopalmar extension of 3 mm and corresponds to the slow leakage of contrast medium shown by conventional arthrography. **D** The palmar segment of the SLIL is intact (*white arrows*). It consists of transversely orientated collagen fascicles and provides – together with the dorsal segment – most of the biomechanical strength of the SLIL [7, 8]. Parts of the thin radioscapholunate ligament connecting the palmar radius with the palmar third of the SLIL (*black arrows*) are shown. *R* radius, *S* scaphoid bone, *L* lunate bone

**Table 1** Delineation of scapholunate interosseous ligament (SLIL) segments (*do* dorsal segment, *ce* central segment, *pa* palmar segment)

Delineation	Non-enhanced MRI ( <i>n</i> =41) <i>do/ce/pa</i>	MR arthrography ( <i>n</i> =41) <i>do/ce/pa</i>
Good	7/22/5	39/40/38
Intermediate	29/17/33	2/1/3
Poor	5/2/3	0/0/0

## Results

Plain radiography showed signs of static carpal instability in two patients, both of whom had dorsal intercalated segment instability (DISI) deformities and a scapholunate (SL) joint space widened to 4 mm and 5 mm on static views, respectively. In eight other patients the SL joint space was slightly widened to 2.5–3.0 mm; four of these showed definite widening (>3 mm) with stress views.

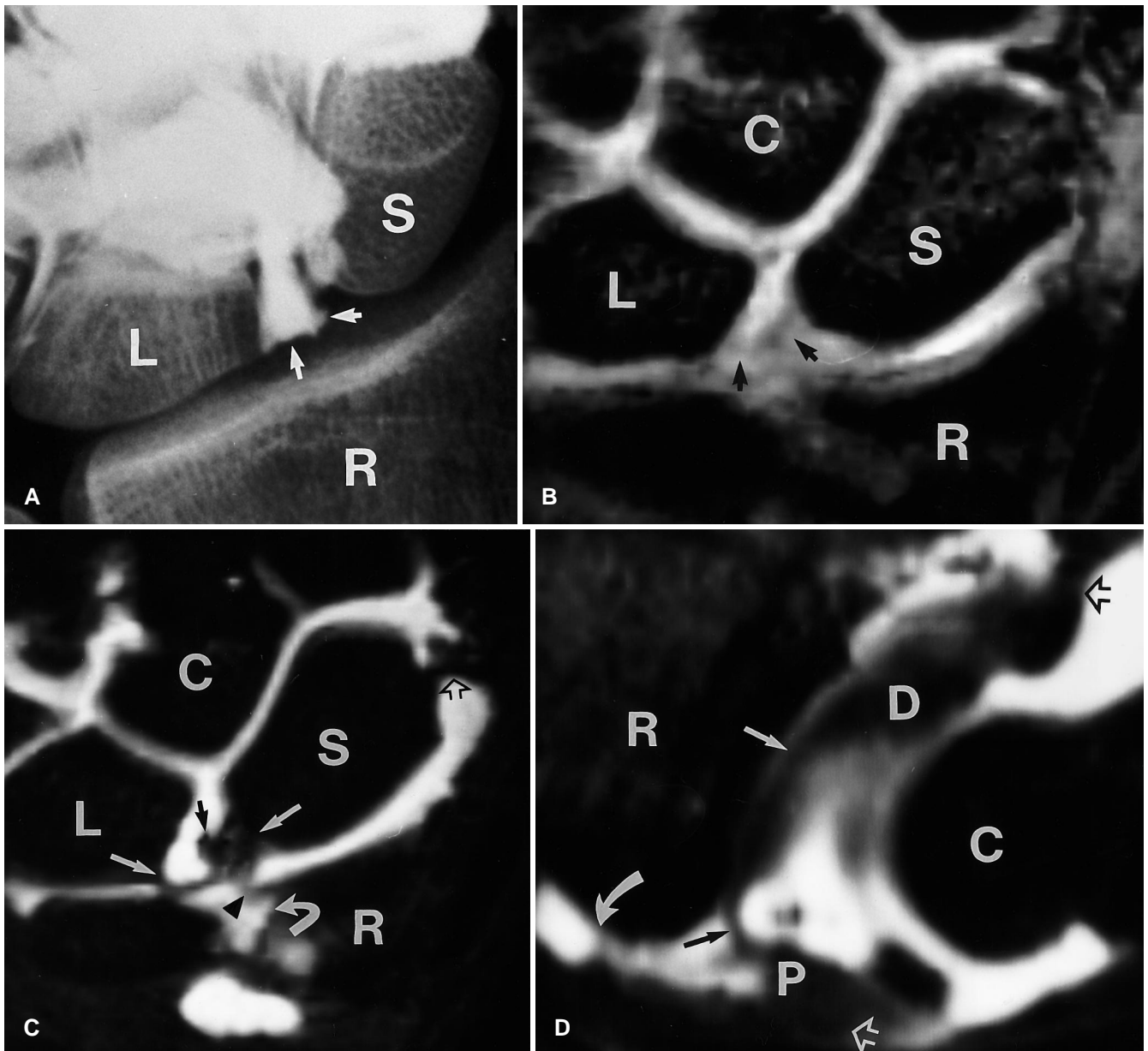


**Fig. 2A–D** A 24-year-old man with a history of recurrent wrist trauma who complained of radial pain. **A** Arthrogram, obtained after a midcarpal injection, shows contrast material filling the slightly widened scapholunate joint (*arrows*). However, no leakage through the SLIL could be demonstrated. **B** Non-enhanced MRI shows areas of inhomogeneously high signal intensity (*arrows*) between the scaphoid and lunate bones, which was interpreted as a rupture of the SLIL. **C** MR arthrography at the transition of the SL interosseous membrane and the palmar segment of the SLIL shows an extremely elongated ligament. The elongated palmar aspect of the SL interosseous membrane is attached to the lunate bone and the scaphoid bone (*white arrows*); the inhomogeneous tissue in between corresponds to scar tissue (*black arrow*). Addi-

tionally, part of the radioscapulunate ligament (*arrowhead*) and the palmar radial recessus (*curved arrow*) are shown. The ligament carrying the main vascular supply to the scaphoid is intact (*open arrow*). **D** Sagittal reconstruction through the SL joint shows the strong dorsal (*D*) and palmar (*P*) parts of the SLIL and the elongated thin interosseous membrane (*arrows*). The attachments of the dorsal SLIL to the dorsal capsular ligaments (*black open arrow*) and the palmar SLIL to the palmar capsular ligaments (*white open arrow*) are marked. Contrast medium right of the SLIL is located in the mid-carpal joint, left of it in the radiocarpal joint. Note the palmar radial recessus (*curved arrow*). *R* radius, *S* scaphoid bone, *L* lunate bone, *C* capitate bone, *D* dorsal SLIL, *P* palmar SLIL.

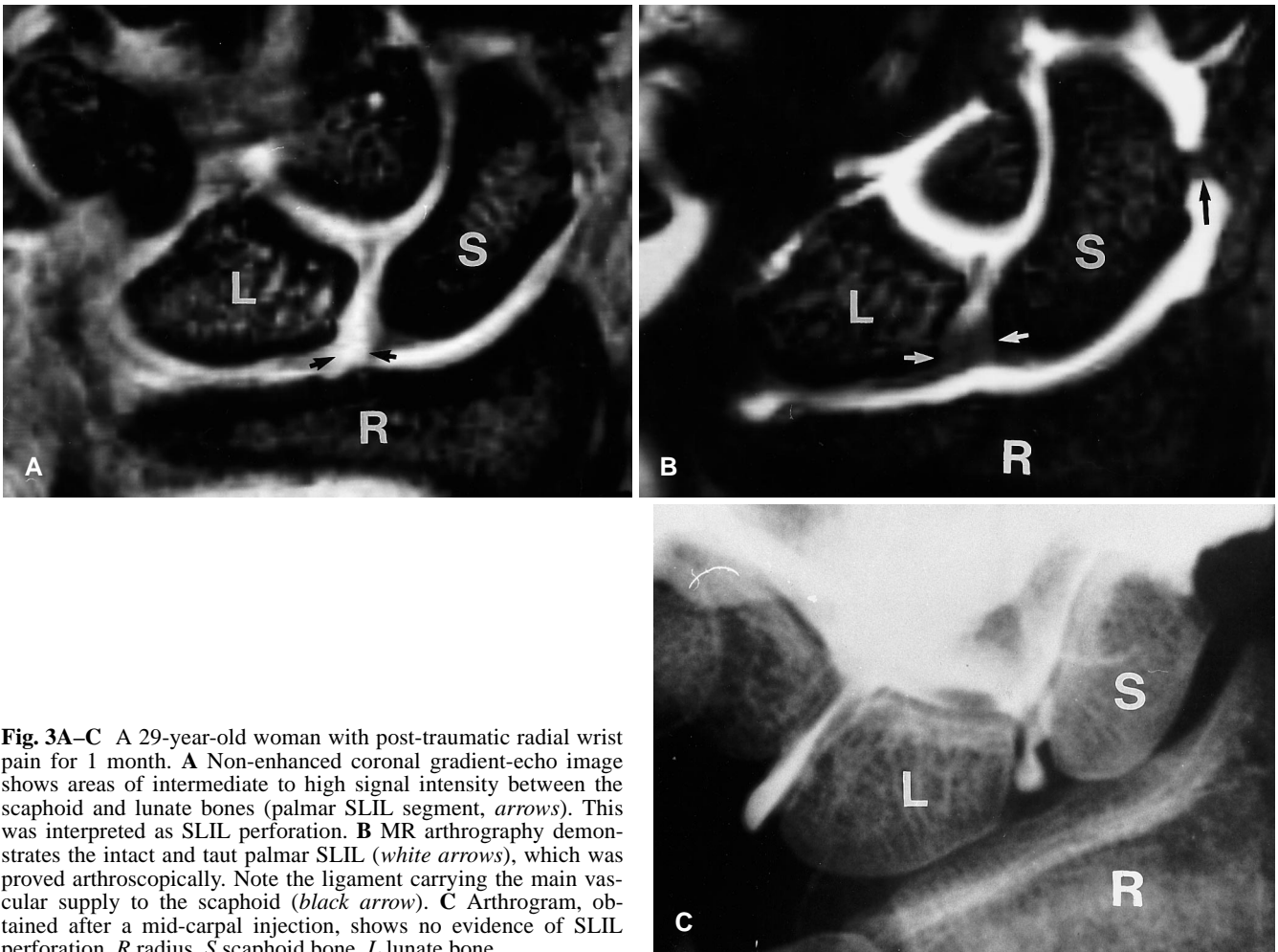


**Fig. 3A–C** A 29-year-old woman with post-traumatic radial wrist pain for 1 month. **A** Non-enhanced coronal gradient-echo image shows areas of intermediate to high signal intensity between the scaphoid and lunate bones (palmar SLIL segment, *arrows*). This was interpreted as SLIL perforation. **B** MR arthrography demonstrates the intact and taut palmar SLIL (*white arrows*), which was proved arthroscopically. Note the ligament carrying the main vascular supply to the scaphoid (*black arrow*). **C** Arthrogram, obtained after a mid-carpal injection, shows no evidence of SLIL perforation. *R* radius, *S* scaphoid bone, *L* lunate bone

All three segments of the SLIL could be identified in 36 of 41 wrists (88%) by non-enhanced MRI and in all patients by MR arthrography (Table 1, Fig. 1).

The average SLIL length in the dorsopalmar direction was  $12.8 \pm 0.3$  mm measured by non-enhanced MRI and  $13.6 \pm 0.4$  mm by MR arthrography.

Signal intensity was evaluated for 123 SLIL segments (41 dorsal, 41 central and 41 palmar segments) of 41 SL joints (Table 2). With non-enhanced MRI, absent signal intensity (type 1) was found in 13 of 41 of the dorsal, 8 of 41 of the central and 10 of 41 of the palmar SLIL segments, type 2 signal intensity in 11 of 41 of the dorsal, 12 of 41 of the central and 18 of 41 of the palmar SLIL segments, type 3 signal intensity in 6 of 41 of the dorsal, 4 of 41 of the central and 4 of 41 of the palmar SLIL segments and type 4 signal intensity in 2 of 41 of the dorsal, 6 of 41 of the central and 2 of 41 of the palmar SLIL segments (Figs. 1–3). Type 5 signal intensity (linear intermediate signal intensity traversing both the proximal and distal surface) was found in 9 of 41 of the dorsal, 11 of 41 of the central and 7 of 41 of the palmar

**Table 2** Signal intensity characteristics of the SLIL on non-enhanced three-dimensional gradient-echo MR images: correlation with wrist arthroscopy. Signal intensity (SI) characteristics (type 1–5) according to Smith [1]: absent signal intensity (type 1), central intermediate signal intensity (type 2), linear intermediate signal intensity traversing the distal surface only (type 3), linear intermediate signal intensity traversing the proximal surface only (type 4) or linear intermediate signal intensity traversing both the proximal and distal surfaces of the SLIL (type 5). (*n*, total number of SLIL segments with SI type 1–5; +, number of SLIL defects proved arthroscopically; –, number of intact SLIL proved arthroscopically)

Signal intensity characteristics	Dorsal SLIL <i>n</i> (+/–)	Central SLIL <i>n</i> (+/–)	Palmar SLIL <i>n</i> (+/–)
SI type 1	13 (0/13)	8 (1/7)	10 (1/9)
SI type 2	11 (1/10)	12 (3/9)	18 (4/14)
SI type 3	6 (1/5)	4 (2/2)	4 (2/2)
SI type 4	2 (0/2)	6 (1/5)	2 (1/1)
SI type 5	9 (2/7)	11 (7/4)	7 (3/4)

**Table 3** Diagnostic confidence rates for evaluation of the SLIL (*do* dorsal segment, *ce* central segment, *pa* palmar segment)

Confidence	Non-enhanced MRI ( <i>n</i> =41)	MR arthrography ( <i>n</i> =41)
	<i>do/ce/pa</i>	<i>do/ce/pa</i>
Certainly normal	13/11/9	32/24/27
Probably normal	11/6/12	4/1/2
No assessment possible	8/7/7	0/0/0
Probably pathological	6/6/8	1/1/3
Certainly pathological	3/11/5	4/15/9

**Table 4** SLIL pathology evaluated by non-enhanced MRI versus MR arthrography: correlation with wrist arthroscopy. True positive and true negative rates were calculated from definitely normal/pathological confidence ratings. Numbers in parentheses are numbers of SLIL defects proved arthroscopically. (*do* dorsal segment, *ce* central segment, *pa* palmar segment)

	Non-enhanced MRI ( <i>n</i> =41)	MR arthrography ( <i>n</i> =41)
	<i>do/ce/pa</i>	<i>do/ce/pa</i>
True positive	2 (4)/9 (14)/4 (11)	4 (4)/14 (14)/8 (11)
True negative	13 (37)/11 (27)/8 (30)	32 (37)/23 (27)/27 (30)

SLIL segments with non-enhanced MRI (Table 2, Figs. 2B, 3A).

Table 1 shows delineation rates for the different SLIL segments. MR arthrography allowed good delineation of all SLIL segments in 95% (117/123), non-enhanced MRI in 28% (34/123) ( $P < 0.001$ , chi-squared) (Figs. 1–3).

The SLIL was evaluated with a high confidence level (certainly normal or certainly pathological) in 52 of 123 (42%) segments with non-enhanced MRI and in 111 of 123 (90%) segments with MR arthrography ( $P < 0.001$ , chi-squared, Table 3). With non-enhanced MRI 22 of 123 (18%) SLIL segments could not be assessed (confidence level 3); with MR arthrography all SLIL segments could be assessed in all patients (Table 3, Figs. 1–3).

With conventional three-compartment wrist arthrography 26 wrists showed no abnormality of the SLIL, and 19 wrists had a pathological leakage through the SLIL from the mid-carpal into the radiocarpal joint.

Wrist arthroscopy demonstrated defects of the SLIL in 17 patients. Six defects were shown only in the central and 3 only in the palmar part of the ligament. In 4 patients there were combined defects of the central and palmar parts, and in 4 patients the whole ligament was torn.

Signal intensity characteristics for the SLIL on non-enhanced images showed a high negative predictive value regarding type 1 signal intensity: 13 of 13 (100%) for the dorsal, 7 of 8 (88%) for the central and 9 of 10 (90%) for the palmar SLIL segment. However, signal intensities type 2–5 did not correlate well with findings from arthroscopy (Table 2).

Compared with arthroscopy, non-enhanced MRI was able to classify SLIL defects as definitely positive in 2 of 4 cases for the dorsal, 9 of 14 for the central and 4 of 11 for the palmar segments. This results in an overall true positive rate of 52% for definitely detecting and localizing defects. MR arthrography had a true positive rate of 90% for classifying defects of the three different parts of the SLIL (Table 4). Definite true negative rates were 32 of 94 (34%) for non-enhanced MRI and 82 of 94 (87%) for MR arthrography for all parts of the SLIL together (Table 4).

Sixteen arthrographically positive patients had ligamentous defects shown by arthroscopy. One patient with a partial rupture of the palmar part of the SLIL did not demonstrate a leakage by arthrography. Three patients with slow leakages shown by arthrography did not have defects arthroscopically.

## Discussion

Patients with SLIL defects may be free of symptoms or may have non-specific clinical symptoms and signs. In the latter case they often present with wrist pain and/or instability and may have signs of scaphoid subluxation or even normal findings on plain radiographs, motion and stress views [1, 8, 9, 12, 13]. Arthrographically one may see a communication between the mid-carpal and radiocarpal joint, but it is nearly impossible to distinguish a small, clinically less relevant central SLIL perforation from a possibly relevant SLIL defect in its strong dorsal or palmar parts [7–9, 14]. By providing information about the location and extent of SLIL lesions MR imaging may contribute to the creation of a systematic classification of ligamentous defects and may establish more reliable and predictable treatment methods in the future [6, 7].

MR imaging has been used to evaluate the SLIL and other wrist ligaments in recent years [1, 2, 6, 15–17]. Compared with conventional wrist arthrography sensitivities and specificities of MRI for the diagnosis of SLIL defects have been reported to be between 50% and 95% [2, 15, 17, 18].

As the SLIL forms a small band 18 mm long and 1–6 mm wide extending as a "horseshoe" between the adjacent borders of the scaphoid and lunate [19], it was not possible to consistently visualize all parts of it with the MR imaging techniques used previously [1]. With dedicated receiver coils high spatial resolution images of the SLIL have been reported [6, 18]. Using a 8×8 cm wrist imaging coil with 3D volume acquisition we acquired excellent thin sliced images (0.6–1 mm) of the wrist and its ligaments [10, 11]. For non-enhanced MRI we used a T1-weighted 3D Fourier transform GE sequence with 0.6–1 mm slice thickness similar to that suggested by Totterman et al. [6, 15].

Smith [1] described five types of signal intensity characteristics within the SLIL, which could be reproduced in this study. Whereas Smith evaluated signal intensities for the whole SLIL, we described them for each of the three parts of the SLIL separately in order to characterize each segment of the ligament. Altogether, we found signal intensity type 1 in 25%, type 2 in 33%, type 3 in 11%, type 4 in 8% and type 5 in 22% of all SLIL segments with non-enhanced MRI. This is comparable to Smith's findings concerning types 3, 4 and 5; however, Smith found type 1 signal intensity in 49% and type 2 only in 14% [1]. The difference may be explained by our patient selection: we examined patients with acute and chronic wrist pain, who may have had microtrauma to the ligaments in the past, resulting in areas of fibrous tissue within the SLIL which could have been interpreted as signal intensity type 2 (central intermediate signal intensity). We found type 5 signal intensity in 22% of the SLIL segments (22% of dorsal, 27% of central and 17% of palmar segments), Smith in 19% [1]. Type 5 means a linear intermediate signal intensity completely traversing the SLIL in the sagittal plane and is the pattern which is usually judged as a SLIL perforation. This interpretation, however, results in only 41% true positive and 16% false positive ratings in our study. We did not find signal intensity characteristics helpful, especially for evaluation of the dorsal portion of the ligament (Table 2). Our results underline the statement of Totterman et al. [6] that signal intensity patterns are partly non-specific.

Hajek et al. [20], in a cadaveric study, as well as others [21, 22], demonstrated that depiction of intra-articular structures by MRI can be greatly enhanced by the introduction of contrast material into the joint cavity (Gd-DTPA or simply saline solution). MR arthrography has been successfully used to diagnose ligament, cartilage, soft tissue and capsular pathology in the knee and shoulder [23–25]. In wrist arthrography, the injection of MR contrast medium into the three compartments of the wrist has several advantages. Firstly, the joint cavities of the wrist can be fully expanded. Thus most of the ligamentous and capsular structures are stretched and can be directly visualized and evaluated [10, 11]. Even elongation of the SLIL [19] and other ligaments may be shown and correlated with patterns of instability in the future. Secondly, the high signal of Gd-DTPA leads to an excellent delineation of all parts of the SLIL, which itself has very low or absent signal intensity. Thirdly, MR arthrography has the potential to precisely localize and quantify SLIL leakages, which may have an important impact on future diagnosis and the advancement of new treatment methods [3, 12].

Results of MR wrist arthrography with injection of Gd-DTPA into the radiocarpal joint (Magnevist diluted 1:250 with sterile normal saline solution) were first reported by Schweitzer et al. [16]. He studied 15 patients with chronic wrist pain and reported a sensitivity of

50%, specificity of 86% and accuracy of 77% for detecting SL ligament pathology by MR arthrography (T1-weighted SE sequence, 3 mm slice thickness, 1 mm intersection gap, 256×128 matrix) with arthrography as the standard. However, the prearthrography T1-weighted sequence proved to be even more accurate than MR arthrography.

The present study showed excellent sensitivity (90%) and specificity (87%) for detection and localization of SLIL pathology with thin-sliced GE volumetric imaging. Non-enhanced MRI (3D volume acquisition) resulted in a sensitivity of 52% and a specificity of 34%. One reason for the low sensitivity and specificity of non-enhanced MRI is that 22 of 123 (18%) of the SLIL segments could not be assessed properly; also diagnostic confidence was much lower than with MR arthrography (Table 3).

MR arthrography allowed good delineation of SLIL segments in 95% of cases, non-enhanced MRI in 28%. It was shown that MR arthrography not only exactly delineates normal SLIL segments, as shown by others [1, 6], but, more importantly, also allows exact determination of the site and extent of defects with a high level of confidence.

The SLIL is a complex anatomical structure with at least three separate anatomical zones with different histological properties and biomechanical functions [7, 9, 13, 26]. The palmar and dorsal thirds of the SLIL are true intracapsular, interosseous ligaments with transversely oriented collagen fascicles and provide the ligament with most of its biomechanical strength [7, 9, 13, 19, 26]. The central or proximal third of the SLIL is a thin fibrocartilaginous membrane, that does not provide any stability when the other parts are damaged [7, 9].

By the third decade, asymptomatic age-related attritional perforations begin to appear. These abnormalities increase steadily; by age 50 years, at least 50% of wrists of all people will have lunotriquetral, scapholunate or triangular fibrocartilage perforations demonstrable with arthrography [27, 28]. In cadaveric wrists SLIL defects in a large number of specimens involve the central portion, leaving the dorsal and palmar portions of the ligament intact for stability purposes [7, 9]. Degenerative changes of the SLIL occur slowly and secondary constraints (e.g., extrinsic dorsal and palmar radiocarpal ligaments) prevent degenerative arthritis, joint space widening or DISI deformity from occurring [9]. Bilateral ligament defects (e.g., SLIL defects) have been seen on arthrography [9, 29]. Since these findings have no recognized clinical significance, the future of bilateral demonstration of ligaments is still uncertain.

The exact localization of the leak and measurement of its size may have clinical implications since the success of treatment procedures (e.g., cast immobilization, direct surgical repair, dorsal capsulodesis techniques, partial intercarpal arthrodesis) may depend on a correct diagnosis of the SLIL pathology including ruptures and partial rup-

tures of palmar radiocarpal ligaments and attachments to dorsal and palmar capsular ligaments (Fig. 2D).

Although triple-injection wrist arthrography is still used as the gold standard for SLIL diagnosis, it cannot delineate the site and size of a leak exactly, or show defects in secondary ligamentous constraints. This may explain why many authors found SLIL leakages arthrographically which did not correlate with the precise site of pain in patients with wrist complaints [5, 14, 27, 30, 31]. Whether MR arthrography or even arthroscopy is superior to conventional arthrography for objectively indicating symptomatic defects is still unclear and should be investigated by a valid outcome study after therapy.

Limitations of MR arthrography compared with non-enhanced MRI are its additional cost, invasiveness and the need to inject contrast medium into the joint. The technique is fairly complicated and time-consuming. It takes approximately 2 h to do the prearthrographic MRI, three-compartment wrist arthrography and MR arthrography. Nevertheless, the method was tolerated well by all patients without any need to stabilize the wrist after the procedure. In our opinion the technique is able to delineate most of the intrinsic and extrinsic ligaments of the wrist [10] and may have the potential to replace diagnostic arthroscopy, which has many disadvantages: costs, invasiveness, need to splint the wrist, limited view

of some portions of the ligaments, technical problems [32].

Occult wrist pain is difficult to diagnose accurately. Patients may have subtle histories of trauma and clinical examination that do not result in definitive findings. After plain radiography, instability series, fluoroscopy, motion studies and bone scanning they are referred for arthrography. In these patients triple-injection arthrography may often show SLIL leaks which may not correspond with the location of the patient's wrist pain and may not reveal defects in other wrist ligaments. MR arthrography has the capacity for staging and quantifying SLIL defects and may possibly help to decide whether a defect is biomechanically relevant or a less relevant pin-hole defect in the thin central segment [7, 9] – an abnormality which may exist even in normal young adults and becomes increasingly prevalent with age [28, 29, 33, 34]. Potentially, the pathological significance of degeneration, elongation, pouch formation and defects of the SLIL and secondary ligamentous constraints may be investigated by an outcome study in the future. MR arthrography is able to combine the advantages of conventional three-compartment arthrography and thin-section MRI and may allow the creation of an anatomically based classification of wrist instability syndromes. This should favor the development of more reliable and predictable treatment methods [32].

## References

- Smith DK. Scapholunate interosseous ligament of the wrist: MR appearances in asymptomatic volunteers and arthrographically normal wrists. *Radiology* 1994; 192: 217–221.
- Rominger MG, Bernreuter WK, Kenney PJ, Lee DH. MR imaging of anatomy and defects of wrist ligaments. *Radiographics* 1993; 13: 1233–1246.
- Green DP, Hotchkiss RN. *Operative hand surgery*, 3rd edn. New York: Churchill Livingstone, 1993: 879–888.
- Manaster BJ. The clinical efficacy of triple-injection wrist arthrography. *Radiology* 1991; 178: 267–270.
- Metz VM, Gilula LA. Is this scapholunate ligament normal? *J Hand Surg [Am]* 1993; 18: 746–755.
- Totterman SMS, Miller RJ. Scapholunate ligament: normal MR appearance on three-dimensional gradient-recalled-echo images. *Radiology* 1996; 200: 237–241.
- Berger RA, Imaeda T, Berglund L, An KN, Cooney WP, Amadio PC, Linscheid RL. The anatomic, constraint and material properties of the scapholunate interosseous ligament: a preliminary study. *Adv Biom Hand Wrist* 1994; 9–16.
- Ruby LK, An KN, Linscheid RL, Cooney WP, Chao EYS. The effect of scapholunate ligament section on scapholunate motion. *J Hand Surg [Am]* 1987; 12: 767–771.
- Wright TW, Del Charco MD, Wheeler D. Incidence of ligament lesions and associated degenerative changes in the elderly wrist. *J Hand Surg [Am]* 1994; 19: 313–318.
- Scheck R, Szeimies U, Hierner R, Pfluger T, Wilhelm K, Küffer G. MRT 3-Kompartiment Handgelenksarthrographie: Wertigkeit bei ligamentären und Diskusläsionen. *Zentralband Radiol* 1994; 150, 1–3: 158.
- Scheck R, Kubitzek C, Pfluger T, Hierner R, Wilhelm K, Küffer G. Das karpale scapholunäre Ligament: Darstellung von Normalanatomie, funktioneller Anatomie und pathologischer Veränderungen mit der M3 3-Kompartiment Handgelenksarthrographie. *Radiologie* 1995; [Suppl] 35: 90.
- Adolfsson L. Arthroscopic diagnosis of ligament lesions of the wrist. *J Hand Surg [Br]* 1994; 19: 505–512.
- Meade TD, Schneider LH, Cherry K. Radiographic analysis of selective ligament sectioning at the carpal scaphoid: a cadaver study. *J Hand Surg [Am]* 1990; 15: 855–862.
- Herbert TJ, Faithfull RG, McCann DJ, Ireland J. Bilateral arthrography of the wrist. *J Hand Surg [Br]* 1990; 15: 233–235.
- Totterman SM, Miller R, Wasserman B, Blebea JS, Rubens DJ. Intrinsic and extrinsic carpal ligaments: evaluation by three-dimensional Fourier transform MR imaging. *AJR* 1993; 160: 117–123.
- Schweitzer ME, Brahme SK, Hodler J, Hanker GJ, Lynch TP, Flannigan BD, Godzik CA, Resnick D. Chronic wrist pain: spin-echo and short tau inversion recovery MR imaging and conventional and MR arthrography. *Radiology* 1992; 182: 205–211.

17. Gundry CR, Kursunoglu-Brahme S, Schwaighofer B. Is MR better than arthrography for evaluating the ligaments of the wrist? In vitro study. *AJR* 1990; 154: 337-341.
18. Zlatkin MB, Chao PC, Osterman AL, Schnall MD, Dalinka MK, Kressel HY. Chronic wrist pain: evaluation with high-resolution MR imaging. *Radiology* 1989; 173: 723-729.
19. Boabighi A, Kuhlmann JN, Kenesi C. The distal ligamentous complex of the scaphoid and the scapho-lunate ligament: an anatomic, histological and biomechanical study. *J Hand Surg [Br]* 1993; 18: 65-69.
20. Hajek PC, Baker LL, Sartoris DJ, Neumann CH, Resnick D. MR arthrography: anatomic-pathologic investigation. *Radiology* 1987; 164: 141-7.
21. Hajek PC, Sartoris DJ, Neumann CH, Resnick D. Potential contrast agents for MR arthrography: in vitro evaluation and practical observations. *AJR* 1987; 149: 97-104.
22. Engel A. Magnetic resonance knee arthrography. *Acta Orthop Scand* 1990; 240 [Suppl]: 3-57.
23. Burk DL, Karasick D, Kurtz AB, Mitchell DG, Rifkin MD, Miller CL, Levy DW, Fenlin JM, Bartolozzi AR. Rotator cuff defects: prospective comparison of MR imaging with arthrography, sonography, and surgery. *AJR* 1989; 153: 87-92.
24. Flannigan B, Kursunoglu-Brahme S, Snyder S, Karzel R, Del Pizzo W, Resnick D. MR arthrography of the shoulder: comparison with conventional MR imaging. *AJR* 1990; 155: 829-832.
25. Palmer WE, Brown JH, Rosenthal DI. Rotator cuff: evaluation with fat-suppressed MR arthrography. *Radiology* 1993; 188: 683-687.
26. Berger RA, Blair WF, Crowinshield RD, Flatt AE. The scapholunate ligament. *J Hand Surg* 1982; 1: 87-91.
27. Levinsohn EM, Rosen ID, Palmer AK. Wrist arthrography: value of the three-compartment injection method. *Radiology* 1991; 179: 231-239.
28. Mikic Z. Arthrography of the wrist joint: an experimental study. *J Bone Joint Surg AM* 1984; 66: 371-384.
29. Viegas SF, Patterson RM, Hokanson JA, Davis J. Wrist anatomy: incidence, distribution, and correlation of anatomic variations, tears, and arthrosis. *J Hand Surg [Am]* 1993; 18: 463-475.
30. Manaster BJ, Mann RJ, Rubenstein S. Wrist pain: correlation of clinical and plain film findings with arthrographic results. *J Hand Surg* 1987; 12-A: 495-503.
31. Metz VM, Mann FA, Gilula LA. Three-compartment wrist arthrography: correlation of pain site with location of uni- and bidirectional communications. *AJR* 1993; 160: 819-822.
32. North ER, Thomas S. An anatomic guide for arthroscopic visualization of the wrist capsular ligaments. *J Hand Surg [Am]* 1988; 13: 815-822.
33. Mikic ZD. Age changes in the triangular fibrocartilage of the wrist joint. *J Anat* 1978; 126: 367-384.
34. Viegas SF, Ballantyne G. Attritional lesions of the wrist joint. *J Hand Surg [Am]* 1987; 12: 1025-1029.